Microwave-assisted synthesis to prepare metal-organic framework for luminescence thermometry

Alia Mansar, Hélène Serier-Brault

Microwave-assisted synthesis to prepare metal-organic framework for luminescence thermometry

Alia Mansar, Hélène Serier-Brault[*]

Université de Nantes, CNRS, Institut des Matériaux Jean Rouxel, IMN, F-44000 Nantes, France

ABSTRACT

The lanthanide metal-organic framework, $La_{1.23}Na_{0.30}(1,3\text{-BDC})_2(H_2O)\cdot 4H_2O$ (1,3-BDC: 1,3-benzenedicarboxylate), has been for the first time synthesized under microwave-assisted hydrothermal conditions with a synthesis duration of 5 minutes. The substitution of La^{3+} by Eu^{3+} and Tb^{3+} was possible until a maximal content of 10%.mol and the investigation of luminescence properties reveals that emitting cations can be located in the chains formed by the LnO_{10} polyhedra but also into the polar channels proposed by the structure, where some La^{3+} crystallographic sites are also available. Finally, when codoped by Eu^{3+} and Tb^{3+}, the materials exhibit thermometric properties in the cryogenic range with a maximal relative thermal sensitivity around 1% K^{-1} at 80K.

1.INTRODUCTION

Lanthanide-based MOFs (LnMOFs) are considered as promising functional materials for optical properties, especially due to their luminescent properties that can be used for applications such as chemical or temperature sensing, lightings, displays [1,2,11,12,3–10]… In our group, we have been working for several years on LnMOFs for luminescence thermometry [13–15] which, compared to conventional contact thermometry, has unique and distinct advantages of fast response, high accuracy, being non-invasive and presenting high spatial resolution (typically submicron scale) where traditional methods are ineffective.[16–18] Among the diverse aspects to Ln^{3+}-based luminescent thermometry, one of the most robust methodologies relies on the measurement of the intensity of two transitions of distinct Ln^{3+} emitting centers. For mixed-metal LnMOFs, the temperature is most often determined from the ratio between the intensity of the $^5D_4 \rightarrow {}^7F_5$ and of the $^5D_0 \rightarrow {}^7F_2$ transitions of Tb^{3+} and Eu^{3+}, respectively.[3,19,20]

The application of microwave heating in synthetic chemistry starts during the late 1980s.[21] This technique has been proposed as an alternative to conventional hydro- or solvothermal reactions due to several advantages: (i) energy efficiency, (ii) fast crystallization (increment in number of reaction sites), (iii) phase selectivity, (iv) high yields, (v) variety of morphologies, (vi) particle size control, (vii) lower temperatures and reaction times. Although microwave heating was first used for the synthesis of inorganic materials, this technique has been also developed for the synthesis of MOFs.[22–27]

In our group, we have worked, during the last couple of years, on different MOFs[13,28] built upon the same organic ligand, namely 1,3-BDC (1,3-benzene dicarboxylic acid or isophthalic acid), and with Eu^{3+} and Tb^{3+} as cations in order to elaborate luminescent thermometers. Our first

compound[13], $[Tb_{0.87}Eu_{0.13}(1,3\text{-}BDC)_3(H_2O)_2]\cdot H_2O$, exhibits a crystal structure where Ln^{3+} polyhedral form dimers connected by organic linkers to, subsequently form helix chains. The material was performant as a cryogenic luminescent thermometer with a relative thermal sensitivity of 3.26% K^{-1} at 35.5 K. In a second investigation, we were focused on a series of mixed compounds, $[Tb_{1-x}Eu_x(CH_3COO)(1,3\text{-}BDC)(H_2O)]$[28], where the Ln^{3+} polyhedra form also dimers but in a tridimensional network. In this study, we highlighted the role of the Eu/Tb ratio to tune the thermal sensitivity of the thermometers which were, in that case, sensitive in the physiological range (around 300K). To pursue our investigation of the role of inorganic network in LnMOFs on the thermometric properties while maintaining the same organic ligand, we herein investigate a new LnMOF that we recently discovered, namely $Ln_{1.14}Na_{0.57}(BDC)_2(H_2O)\cdot 4H_2O$ (Ln = La, or Ce).[29] In this material, the inorganic network is composed by LnO_{10} polyhedra connected to form infinite chains linked by the organic linkers. Moreover, the crystal structure exhibits non-polar and polar channels, the latter one being filled by Ln^{3+} and Na^+ cations. Consequently, we report in this work the microwave synthesis of this new MOF in order to reduce the synthesis time and we have investigated the doping of the La counterpart by Eu^{3+} and Tb^{3+} to elaborate new luminescent thermometer.

2. EXPERIMENTAL SECTION

2.1 Materials and synthesis

Reagents and Chemicals: $La(NO_3)_3$, $6H_2O$ (99.99%), $Tb(NO_3)_3\cdot 6H_2O$ (99.99%), $Eu(NO_3)_3\cdot 6H_2O$ (99.99%), and isophtalic acid (99%) were purchased from Alfa Aesar. All chemicals were used without further purification.

Synthesis of LaMOF. 1,3-H_2BDC (86 mg, 0.52 mmol) was dissolved in 0.6 mL of an aqueous NaOH solution (1.5 M) and in 10 mL H_2O while $La(NO_3)_3 \cdot 6H_2O$ (113 mg, 0.26 mmol) was dissolved in 2 mL of dezionized water. The cationic solution was added dropwise in the ligand solution under stirring and a white precipitate was formed. The pH of the mixture was measured at equal to 4.7. Then, the above mixture was placed in a sealed 35 mL borosilicate glass vessel, which was heated in a Discover SP CEM microwave. White powder was obtained. Yield: 67.6%. Anal. Calcd for $La_{1.23}Na_{0.30}C_{16}O_{13}H_{18}$ (%): C, 32.23; H, 3.02. Found: C, 32.06; H, 3.35. IR (KBr pellet, cm^{-1}): 1668 (sh),1612 (vs), 1599 (vs), 1541 (vs), 1510 (s), 1475 (s), 1452 (vs), 1389 (vs), 1315 (m), 1275 (m), 1155 (m), 1072 (m), 924 (m), 820 (m), 743 (s), 710 (s), 658 (m), 569 (m), 519 (m) and 422 (m).

Synthesis of LaMOF-5Eu-5Tb and LaMOF-7Eu-3Tb. The procedure was the same as that for **NaLaMOF** except that the cationic solution was composed by $La(NO_3)_3 \cdot 6H_2O$ (101 mg, 0.234 mmol), $Eu(NO_3)_3 \cdot 6H_2O$ (5.56 mg, 0.013 mmol), and $Tb(NO_3)_3 \cdot 6H_2O$ (5.88 mg, 0.013 mmol) for **LaMOF-5Eu-5Tb** and by $La(NO_3)_3 \cdot 6H_2O$ (101 mg, 0.234 mmol), $Eu(NO_3)_3 \cdot 6H_2O$ (6.79 mg, 0.023 mmol), and $Tb(NO_3)_3 \cdot 6H_2O$ (3.53 mg, 0.0078 mmol) for **LaMOF-7Eu-3Tb**. Both samples were synthesized at 170°C/15 min in a Discover SP CEM microwave. Anal. Calcd for **LaMOF-5Eu-5Tb,** $La_{1.107}Eu_{0.06}Tb_{0.06}Na_{0.30}C_{16}O_{13}H_{18}$ (%): C, 32.12; H, 3.01. Found: C, 32.19; H, 3.52. Anal. Calcd for **LaMOF-7Eu-3Tb,** $La_{1.107}Eu_{0.086}Tb_{0.037}Na_{0.30}C_{16}O_{13}H_{18}$ (%): C, 32.13; H, 3.01. Found: C, 32.77; H, 3.31. The Eu and Tb contents (in percentage) were determined by ICP-AES to be equal to 48.7/51.3 and 70.1/29.9 **LaMOF-5Eu-5Tb** and **LaMOF-7Eu-3Tb,** respectively.

2.2 Characterization

Powder X-ray Diffraction spectra were monitored using a D8 Bruker diffractometer in the Bragg-Brentano geometry, equipped with a front germanium monochromator, a copper anode ($Cu_{K\text{-}L3}$ radiation λ=1.540598 Å) and a LynxEye PSD detector. The simulated pattern was obtained by the PowderCell 2.4 software from the cif file of the **LaMOF** compound (CCDC 2013538). Thermogravimetric analyses (TGA) were performed by flowing dry air with a heating and cooling rate of 5°C/min on a SETARAM TG-DSC 111 between 20 and 800°C. Fourier transform infrared (FT-IR) spectra were recorded in the 4000-400 cm^{-1} range on a Bruker Vertex FTIR spectrometer equipped with a computer control using the OPUS software. For ICP-AES analyses, samples were dissolved in a 10% HNO_3 solution and analyzed by ICP-AES. The calibration curve was established from the analysis of five standard solutions containing Na, La, Eu and Tb in various contents to cover a range in accordance with targeted concentrations. The standard solutions were prepared with high purity monoelemental solutions in acidic solution. Photoluminescence spectra were recorded on a Jobin-Yvon Fluorolog 3 fluorometer equipped with a photomultiplier (excitation source: 450 W Xe arc lamp) using the front face acquisition mode. The emission spectra were corrected for detection and optical spectral response of the spectrofluorimeter and the excitation spectra were weighed for the spectral distribution of the lamp intensity using a photodiode reference detector. The temperature-dependent photoluminescence measurements were recorded on the same spectrometer controlling the temperature by a cryostat coupled with the Fluorolog cooled by liquid nitrogen. Lifetimes measurements were measured with the same equipment but the excitation was performed by a UV Xenon flash tube while the time-dependence of the emission was recorded with the photomultiplier. The morphology of powder was

investigated with a field-emission gun scanning electron microscope JEOL JSM7600F operating at 7 kV.

3. RESULTS AND DISCUSSION

3.1 Microwave synthesis

The compound **LaMOF** crystallizes in the tetragonal apolar space group $P4_22_12$.[29] In the network, each La^{3+} cation is coordinated by ten oxygen atoms, eight oxygen atoms arising from the two different carboxylate groups and two oxygen atoms from water molecules in a distorted bicapped square prismatic environment. The LaO_{10} coordination polyhedra are connected by a triangular face along the *c* axis to form infinite chains. Subsequently, each chain is linked to four others chains by the BDC^{2-} ligand with a distance between metal centers equal to 11.231(1) Å along the *a* axis (to form a 3D MOF network with channels running along the *c* axis (Figure 1a).

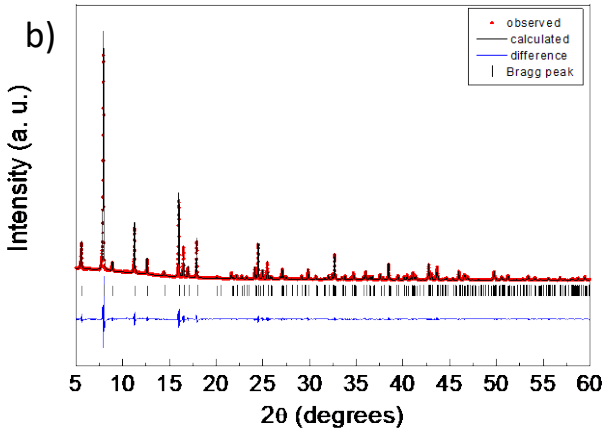

Figure 1. a) projection along the *c* axis of the **LaMOF** structure (blue: LaO_{10} polyhedra, red: oxygen, yellow: sodium, grey: carbon, H atoms being omitted for clarity). b) Le Bail refinement

of **LaMOF** synthesized at 170°C/5 min (C = 0.02 M, M/L = 2) by microwave-assisted hydrothermal route.

The synthesis of **LaMOF** by microwave-assisted hydrothermal synthesis was performed for a concentration of [La^{3+}] equal to 0.02 mol/L and a Metal/Ligand ratio of 1:2. In a first step, the isophthalic ligand was dissolved by a stoichiometric quantity of a NaOH aqueous solution to reach a pH varying from 5 to 5.3 after the whole dissolution. Then the cationic solution was added dropwise to form a white powder, and the pH decreases to around 4.8. Finally, the mixture is placed the microwave oven. The system was investigated for three different temperatures, 150, 160 and 170°C, and for four synthesis durations (5, 15, 30 and 60 min) (Figure 2). For a temperature of 150°C and whatever the synthesis time, the obtained phase corresponds to the precursor already reported in our previous work,[29] which actually is the initial white precipitate that one formed by adding the cationic solution to the basic solution of ligand. At 160°C, the **LaMOF** material is obtained only for a synthesis time of 60 min, for lower duration a mixture with precursor is obtained. Finally, at 170°C the **LaMOF** compound is obtained only after 5 minutes (figure 2b). Le Bail refinement of this compound was performed to confirm the purity of the phase (Figure 1b).

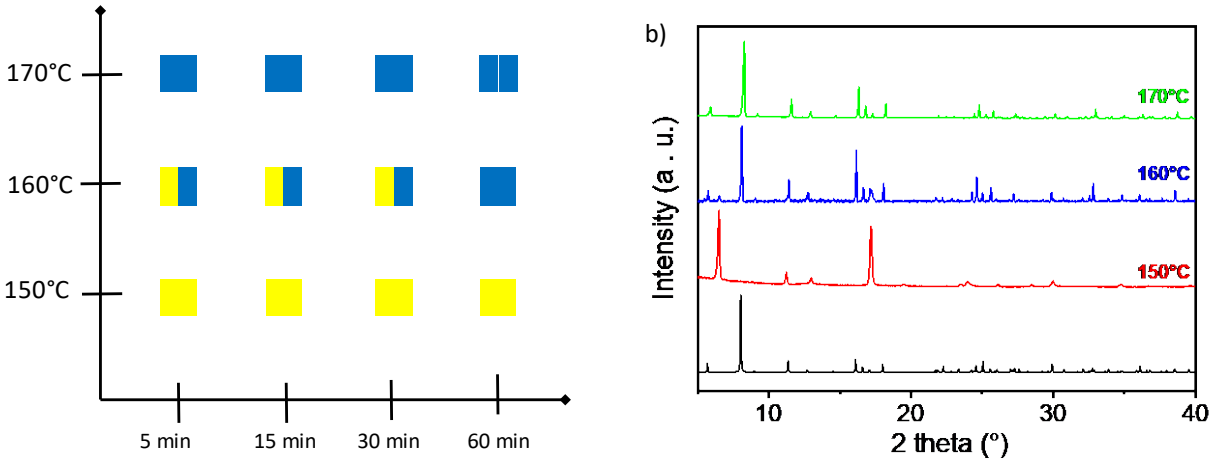

Figure 2. a) Schematic diagram of obtained phases according the synthesis parameters (yellow color correspond to the precursor phase and blue color to the **LaMOF**). b) X-ray patterns of the **LaMOF** compound obtained by microwave-assisted hydrothermal route at different temperatures (t = 5 min, C = 0.02 M, M/L = 2), the black line corresponds to the simulated X-ray pattern of **LaMOF** (CCDC 2013538).[29]

In our previous work where samples were synthesized by conventional hydrothermal route (180°C/5 days), we highlighted the presence of Na^+ cations in the structure originated from the use of sodium hydroxide solution to dissolve the organic ligand. Then, we concluded to a final chemical composition of $La_{1.14}Na_{0.57}(1,3\text{-}BDC)_2(H_2O)\cdot 4H_2O$, where polar channels exhibited by the crystal structure are occupied by disordered Ln^{3+} and Na^+ cations surrounded by water molecules. Here, we decided to add NaOH solution in a stoichiometric way to dissolve the ligand, which leads to a concentration ten times smaller (9.10^{-3} M) and a final chemical composition (determined by ICP analyses) of $La_{1.23}Na_{0.30}(1,3\text{-}BDC)_2(H_2O)\cdot 4H_2O$. Consequently, the La/Na in the final compound can be modulated by varying the amount of Na^+ during the synthesis.

The morphology of the **LaMOF** obtained at 170°C/5 min was assessed by SEM analyses to identify the effect of the time synthesis reduction on the grain size. Therefore, SEM analyses evidence the formation of micro-rods with an average width of 1 µm and an average length of 10 µm (Figure 3). Consequently, the microwave-assisted hydrothermal route enables to get the phase **LaMOF** in very short synthesis time (5 min) but the use of relatively high temperature, i.e. 170°C, do not allow to obtain of nanopowder in these conditions.

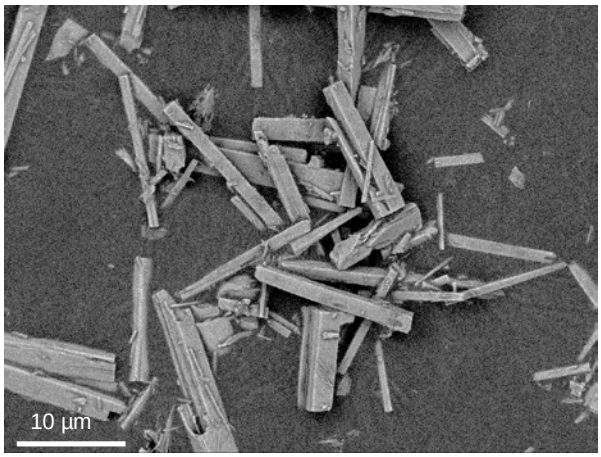

Figure 3. SEM photograph of **LaMOF** synthesized at 170°C/5 min (C = 0.02 M, M/L = 2) by microwave-assisted hydrothermal route.

The doped **LaMOF** material, namely **LaMOF-5Eu-5Tb** and **LaMOF-7Eu-3Tb**, where also prepared by microwave-assisted hydrothermal route at 170°C but the time duration was increased to 15 min to get pure phase. Both PXRD analysis (Figures S1 and S2) and FT-IR spectroscopy (Figure S3) confirmed the mixed Eu–Tb compounds are isostructural to undoped **LaMOF**[29]. Thermogravimetric (Figure S4) and elemental analyses confirmed the chemical compositions. Moreover, the Tb:Eu molar ratio was determined to high precision by taking ICP-AES measurements (Table S1).

3.2 Luminescence properties

The photophysical properties at room temperature of both **LaMOF-5Eu-5Tb** and **LaMOF-7Eu-3Tb** were thoroughly investigated. As reported in our previous work[29], the **LaMOF** host lattice can be easily doped by small content of the optically active ions Eu^{3+} and Tb^{3+} to provide white luminescence. Herein, the total amount of luminescent ions was fixed at 10 mol. %, which

corresponds to the thermodynamic solubility limit in the framework, and two Eu/Tb ratio were tested, namely 1:1 and 1:0.42. Excitation spectra were monitored at room-temperature within the $^5D_0 \rightarrow {}^7F_2$ Eu^{3+} transition (λ_{em} = 614 nm), and the $^5D_4 \rightarrow {}^7F_5$ Tb^{3+} (λ_{em} = 542 nm) but also within the ligand broad emission at λ_{em} = 394 nm (Figures S5 and S6). The excitation band of the organic ligand, which is centered at 342 nm, is present on excitation spectra monitored at 614 and 542 nm but with a moderate intensity, the main excitation peak being centered at 297 nm for λ_{em} = 614 nm (Eu^{3+} emission) and at 322 nm for λ_{em} = 542 nm (Tb^{3+} emission). This second excitation band, located at higher energy than the ligand one, can be assigned to a O-Ln^{3+} charge transfer, indicating that emitting lanthanides are also placed into MOF channels, surrounded by the water molecules.[30,31] The presence of this charge transfer band indicates the possibility to excite, in a separate way, the emitters located in the LnO_{10} chains of the network and those placed in the MOF channels (Figure 1).

The phosphorescence spectrum at 77 K (Figure S7) of **LaMOF** was recorded to identify the lowest-lying triplet energy state positioning of the organic ligands. Contrary to what expected, the phosphorescence spectrum is composed by two broad bands peaking at 394 nm and 477 nm, respectively. The peak centered at high energy was assigned to the $S_1 \rightarrow S_0$ transition as confirmed by the fluorescence spectrum of **LaMOF** recorded at 300K, while the peak centered at 477 nm corresponds to the $T_1 \rightarrow S_0$ transition. Time-resolved spectroscopy was used to precisely determine the triplet energy (Figure S8), and consequently, the triplet level can be estimated to be 22200 cm^{-1} from the shortest-wavelength, which is in a suitable energy range to sensitize both Eu^{3+} and Tb^{3+} according to the Latva's empirical rule.[32]

The solid-state luminescence of **LaMOF-5Eu-5Tb** and **LaMOF-7Eu-3Tb** was investigated at room temperature for the three different excitation wavelengths. Under UV irradiation, the emission spectra of **LaMOF-5Eu-5Tb** (Figure S9) and **LaMOF-7Eu-3Tb** (Figure S10) display the characteristic green and red luminescence of Tb^{3+} and Eu^{3+} ions, respectively, which exhibit typical lines at 490, 545, 581, and 619 nm and at 587, 611, 652, and 695 nm, attributed to the Tb^{3+} $^5D_4 \rightarrow {}^7F_{6\text{-}3}$ transitions and the Eu^{3+} $^5D_0 \rightarrow {}^7F_{0\text{-}4}$ transitions, respectively. The main effect of excitation wavelength changes concerns the ligand emission, which is present at λ_{exc} = 322 or 342 nm whereas it is totally absent et λ_{exc} = 297 nm, in agreement with excitation spectra. Thus, under excitation at 322 or 342 nm, both materials exhibit almost white luminescence with CIE parameters close to (0.33; 0.33) (Figure S11, and Table S2) as already reported while at λ_{exc} =297 nm, the blue contribution brought by the ligand disappeared to generate orange and red emitters.

This shift in the color coordinates is due to the Tb^{3+}-to-Eu^{3+} energy transfer, which was evidenced by the presence of $^7F_6 \rightarrow {}^5D_4$ Tb^{3+} transition (at 483 nm) within the $^5D_0 \rightarrow {}^7F_2$ Eu^{3+} transition in the excitation spectra of a mixed compound (inset in Figures S5 and S6). Nevertheless, the excitation band is very weak, assuming that the Tb^{3+}-to-Eu^{3+} energy transfer is not efficient at room-temperature.

The application of both **Eu-Tb-NaLaMOF** materials as ratiometric luminescent thermometers was characterized using the emission spectra in the 80-250 K range. All thermometry characterizations were performed at λ_{exc} = 297 nm where only the Eu^{3+} and Tb^{3+} emissions are present. As an illustrative example, Figure 4a presents the temperature dependent emission spectra of **LaMOF-7Eu-3Tb** in the 77-250 K range (similar data for the **LaMOF-5Eu-5Tb** material is reported in Figure S12). The temperature dependence of the I_{Tb} (green) and I_{Eu} (red) parameters is

represented in Figure 4b. The integrated areas of the $^5D_4 \rightarrow {}^7F_5$ (I_{Tb}) and of the $^5D_0 \rightarrow {}^7F_2$ (I_{Eu}) emissions were used to define the thermometric parameter as $\Delta = I_{Tb}/I_{Eu}$, I_{Tb} and I_{Eu} being obtained using the emission spectra in the 530–560 nm and 603–633 nm intervals, respectively. In the 80-300K, I_{Tb} and I_{Eu} continuously decrease but the thermal quenching of I_{Tb} is more significant, with a decrease of 75% while I_{Eu} decrease of 30%.

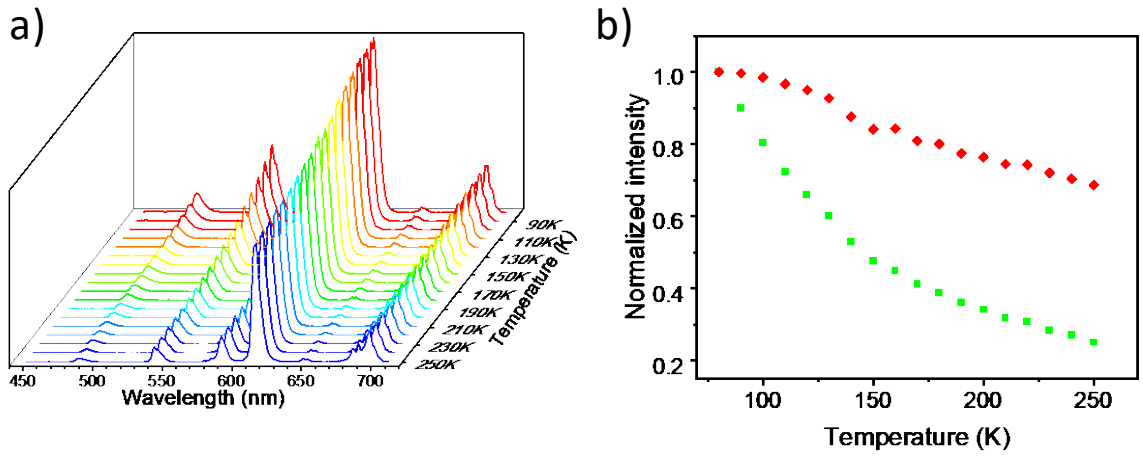

Figure 4. (a) Emission spectra of **LaMOF-7Eu-3Tb** in the 80-300K range with the excitation fixed at 297 nm. (b) Corresponding temperature dependence of I_{Tb} (green) and I_{Eu} (red)

The thermometric parameter Δ of both samples (Figure 5a and Figure S12) is depicted according to the temperature in the 77-250 K range. It may be described by the phenomenological Mott-Seitz expression involving a single deactivation channel assuming a temperature dependence of the Eu^{3+} emission is smaller than that of the Tb^{3+} emission (Figure 4b and Figure S12b) according to the equation (2):[3,13,28]

$$\Delta(T) = \frac{\Delta_0}{1+\alpha \exp(-\Delta E/k_B T)} \qquad (2)$$

where Δ_0 is the Δ parameter at $T \rightarrow 0$ K, $\alpha = W_0/W_R$ is the ratio between the non-radiative and radiative decay rates in the limit of $T \rightarrow 0$ K and ΔE is the energy difference between the emitting level ($^5D_4$) and the level responsible for its non-radiative deactivation. Fitting Equation (2) to the experimental $\Delta(T)$ curves, we find excellent correlation coefficients attesting the adequacy of this simple model to get the calibration curve of the hybrid materials. Finally, the ΔE value was found equal to 161 ± 4 cm^{-1} for **LaMOF-7Eu-3Tb** and 203 ± 3 cm^{-1} for **LaMOF-5Eu-5Tb**. Temperature-dependence of lifetimes where characterized for **LaMOF-7Eu-3Tb** (Figure S14) and it evidences a rapid decrease of the $^5D_4$ decay time between 80 and 300 K while the $^5D_0$ decay time is almost constant. Consequently, the Tb^{3+}-to-Eu^{3+} energy transfer does not govern the thermometric properties. Considering the phosphorescence emission of the ligand (Figures S7 and S8) which overlaps the $^5D_4$ level of Tb^{3+} (487 nm), we can tentatively ascribe the deactivation channel to Tb^{3+}-to-ligand back energy transfer.

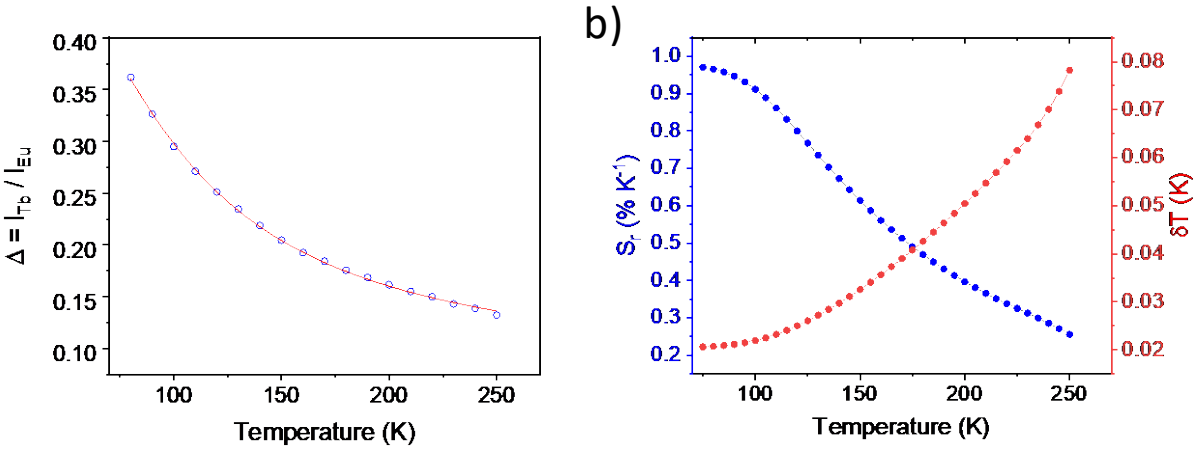

Figure 5. (a) Temperature dependence of Δ in the 80-300K range for **LaMOF-7Eu-3Tb** with excited at 297 nm. The red line represents the calibration curve obtained by the best fit of the

experimental points to equation (2) ($r^2 > 0.999$). (b) Corresponding relative thermal sensitivities and temperature uncertainty (δT) in the same temperature range.

Then, in order to evaluate the thermal performances of mixed compounds, we calculated the relative thermal sensitivity defined as $S_{r=} |\partial\Delta/\partial T|/\Delta$ which is a usual figure of merit to compare the performance of distinct systems.[3,33,34] Both materials exhibit thermal sensitivity in the cryogenic range (< 100 K) with a maximum of relative thermal sensitivity of 0.97 $\%K^{-1}$ at 75 K for **LaMOF-7Eu-3Tb** (Figure 5a**)**, and 0.89 $\%K^{-1}$ at 100 K for **LaMOF-5Eu-5Tb** (Figure S13b). The operating temperature of **LaMOF** when codoped by Eu^{3+} and Tb^{3+} is perfectly in agreement with the chain topology exhibited by the Ln^{3+} polyhedra. Indeed, in the literature, many cryogenic luminescent thermometers based on mixed Eu-Tb MOFs exhibits a chain topology of the inorganic network.[35–37] Thus, the distance Ln-Ln is very short favoring the occurrence of energy transfer between two Ln^{3+} or energy migration.

Finally, the temperature uncertainty $\delta T = 1/S_r \times \delta\Delta/\Delta$, ($\delta\Delta/\Delta$ corresponds to the average error imposed by the photomultiplier detection and was equal to 0.2%) which defines the smallest temperature change that may be ascertained in a given measurement, was evaluated as amounting to 0.02 K for both samples at 80K (Figure 5b and S13b). To evaluate whether the material could be used as a reliable thermometer, cycle tests were performed on **LaMOF-7Eu-3Tb**, and the repeatability was calculated according the equation (3):[13,38]

$$R = 1 - \frac{max|\Delta_c - \Delta_i|}{\Delta_c} \qquad (3)$$

Where Δ_C is the mean thermometric parameter, and Δ_i is the value of each measurement of the thermometric parameter. Then, four cycles between 80 and 150K were carried out (Figure S15) to

get a repeatability R > 97%, which confirms the robustness of the materials for an application as luminescent thermometer.

4. CONCLUSIONS

The **LaMOF** compound can be synthesized by microwave-assisted hydrothermal route with a very short synthesis time (170°C/5 min). The temperature synthesis cannot be decreased below 170°C, which limits the obtaining of nanoparticles. When co-doped by Eu^{3+} and Tb^{3+}, the material can be used as cryogenic luminescent thermometer with a maximum of relative thermal sensitivity of 0.97 $\%K^{-1}$ at 75 K for the **LaMOF-7Eu-3Tb**. As already evidenced in our previous work,[28] an increase of the Eu content has an impact on the thermal sensitivity which is improved.

ASSOCIATED CONTENT

Supporting Information. The following files are available free of charge.

PXRD, Thermal analyses, FTIR, CIE parameters, Luminescence properties (PDF)

AUTHOR INFORMATION

Corresponding Author

* Helene.brault@cnrs-imn.fr

Present Addresses

†If an author's address is different than the one given in the affiliation line, this information may be included here.

Author Contributions

The manuscript was written through contributions of all authors. All authors have given approval to the final version of the manuscript.

ACKNOWLEDGMENT

HB thanks Nicolas Stephant, engineer at the Institute of Matériaux Jean Rouxel of Nantes, for SEM images.

REFERENCES

[1] W.P. Lustig, S. Mukherjee, N.D. Rudd, A. V. Desai, J. Li, S.K. Ghosh, Metal–organic frameworks: functional luminescent and photonic materials for sensing applications, Chem. Soc. Rev. 46 (2017) 3242–3285. https://doi.org/10.1039/C6CS00930A.

[2] F. Artizzu, F. Quochi, A. Serpe, Tailoring functionality through synthetic strategy in hetero-lanthanide, Inorg. Chem. Front. 2 (2015) 213–222. https://doi.org/10.1039/b000000x.

[3] J. Rocha, C.D.S. Brites, L.D. Carlos, Lanthanide Organic Framework Luminescent Thermometers, Chem. - A Eur. J. 22 (2016) 14782–14795. https://doi.org/10.1002/chem.201600860.

[4] Z. Hu, B.J. Deibert, J. Li, Luminescent metal-organic frameworks for chemical sensing and explosive detection, Chem Soc Rev. 43 (2014) 5815–5840. https://doi.org/10.1039/c4cs00010b.

[5] N. Busschaert, C. Caltagirone, W. Van Rossom, P.A. Gale, Applications of Supramolecular Anion Recognition, Chem. Rev. 115 (2015) 8038–8155. https://doi.org/10.1021/acs.chemrev.5b00099.

[6] Y. Cui, F. Zhu, B. Chen, G. Qian, Metal-organic frameworks for luminescence thermometry, Chem. Commun. 51 (2015) 7420–7431. https://doi.org/10.1039/c5cc00718f.

[7] D. Tian, Y. Li, R.Y. Chen, Z. Chang, G.Y. Wang, X.H. Bu, A luminescent metal-organic framework demonstrating ideal detection ability for nitroaromatic explosives, J. Mater. Chem. A. 2 (2014) 1465–1470. https://doi.org/10.1039/c3ta13983b.

[8] X.L. Zhao, D. Tian, Q. Gao, H.W. Sun, J. Xu, X.H. Bu, A chiral lanthanide metal-organic framework for selective sensing of Fe(III) ions, Dalt. Trans. 45 (2016) 1040–1046. https://doi.org/10.1039/c5dt03283k.

[9] P.P. Cui, Y. Zhao, X. Du Zhang, P. Wang, W.Y. Sun, Lanthanide-tricarboxylate frameworks: Synthesis, structure and photoluminescence property, Dye. Pigment. 124 (2016) 241–248. https://doi.org/10.1016/j.dyepig.2015.09.024.

[10] J. Zhao, X. Liu, Y. Wu, D.S. Li, Q. Zhang, Surfactants as promising media in the field of metal-organic frameworks, Coord. Chem. Rev. 391 (2019) 30–43. https://doi.org/10.1016/j.ccr.2019.04.002.

[11] J. Zhao, Y.N. Wang, W.W. Dong, Y.P. Wu, D.S. Li, Q.C. Zhang, A Robust Luminescent Tb(III)-MOF with Lewis Basic Pyridyl Sites for the Highly Sensitive Detection of Metal Ions and Small Molecules, Inorg. Chem. 55 (2016) 3265–3271. https://doi.org/10.1021/acs.inorgchem.5b02294.

[12] Z.S. Qin, W.W. Dong, J. Zhao, Y.P. Wu, Q. Zhang, D.S. Li, A water-stable Tb(III)-based metal-organic gel (MOG) for detection of antibiotics and explosives, Inorg. Chem. Front. 5 (2018) 120–126. https://doi.org/10.1039/c7qi00495h.

[13] I. N'Dala-Louika, D. Ananias, C. Latouche, R. Dessapt, L.D. Carlos, H. Serier-Brault, Ratiometric mixed Eu–Tb metal–organic framework as a new cryogenic luminescent thermometer, J. Mater. Chem. C. 5 (2017) 10933–10937. https://doi.org/10.1039/C7TC03223D.

[14] W. Salomon, A. Dolbecq, C. Roch-Marchal, G. Paille, R. Dessapt, P. Mialane, H. Serier-Brault, A Multifunctional Dual-Luminescent Polyoxometalate@Metal-Organic Framework

EuW10@UiO-67 Composite as Chemical Probe and Temperature Sensor, Front. Chem. 6 (2018) 425. https://doi.org/10.3389/fchem.2018.00425.

[15] C. Viravaux, O. Oms, A. Dolbecq, E. Nassar, L. Busson, C. Mellot-Draznieks, R. Dessapt, H. Serier-Brault, P. Mialane, Temperature sensors based on europium polyoxometalate and mesoporous terbium metal–organic framework, J. Mater. Chem. C. 9 (2021) 8323–8328. https://doi.org/10.1039/d1tc01532j.

[16] C.D.S. Brites, P.P. Lima, N.J.O. Silva, A. Millan, V.S. Amaral, F. Palacio, L.D. Carlos, Thermometry at the nanoscale, Nanoscale. 4 (2012) 4799–4829. https://doi.org/10.1039/C2NR30663H.

[17] O.A. Savchuk, J.J. Carvajal, J. Massons, C. Cascales, M. Aguilo, F. Diaz, Novel low-cost, compact and fast signal processing sensor for ratiometric luminescent nanothermometry, Sensors Actuators, A Phys. 250 (2016) 87–95. https://doi.org/10.1016/j.sna.2016.08.031.

[18] M. Quintanilla, L.M. Liz-Marzán, Guiding Rules for Selecting a Nanothermometer, Nano Today. 19 (2018) 126–145. https://doi.org/10.1016/j.nantod.2018.02.012.

[19] Y. Cui, H. Xu, Y. Yue, Z. Guo, J. Yu, Z. Chen, J. Gao, Y. Yang, G. Qian, B. Chen, A Luminescent Mixed-Lanthanide Metal–Organic Framework Thermometer, J. Am. Chem. Soc. 134 (2012) 3979–3982. https://doi.org/10.1021/ja2108036.

[20] X. Rao, T. Song, J. Gao, Y. Cui, Y. Yang, C. Wu, B. Chen, G. Qian, A highly sensitive mixed lanthanide metal-organic framework self-calibrated luminescent thermometer, J. Am. Chem. Soc. 135 (2013) 15559–15564. https://doi.org/10.1021/ja407219k.

[21] P. Zhu, J. Zhang, Z. Wu, Z. Zhang, Microwave-assisted synthesis of various ZnO hierarchical nanostructures: Effects of heating parameters of microwave oven, Cryst. Growth Des. 8 (2008) 3148–3153. https://doi.org/10.1021/cg0704504.

[22] J. Klinowski, F.A. Almeida Paz, P. Silva, J. Rocha, Microwave-assisted synthesis of metal-organic frameworks, Dalt. Trans. 40 (2011) 321–330. https://doi.org/10.1039/c0dt00708k.

[23] S. Głowniak, B. Szczęśniak, J. Choma, M. Jaroniec, Advances in Microwave Synthesis of

Nanoporous Materials, Adv. Mater. (2021) 2103477. https://doi.org/10.1002/adma.202103477.

[24] H. Liu, Y. Zhao, C. Zhou, B. Mu, L. Chen, Microwave-assisted synthesis of Zr-based metal–organic framework (Zr-fum-fcu-MOF) for gas adsorption separation, Chem. Phys. Lett. 780 (2021) 138906. https://doi.org/10.1016/j.cplett.2021.138906.

[25] A.D.G. Firmino, R.F. Mendes, D. Ananias, S.M.F. Vilela, L.D. Carlos, J.P.C. Tomé, J. Rocha, F.A. Almeida Paz, Microwave Synthesis of a photoluminescent Metal-Organic Framework based on a rigid tetraphosphonate linker, Inorganica Chim. Acta. 455 (2017) 584–594. https://doi.org/10.1016/j.ica.2016.05.029.

[26] K. Behrens, S.S. Mondal, R. Nöske, I.A. Baburin, S. Leoni, C. Günter, J. Weber, H.J. Holdt, Microwave-Assisted Synthesis of Defects Metal-Imidazolate-Amide-Imidate Frameworks and Improved CO2 Capture, Inorg. Chem. 54 (2015) 10073–10080. https://doi.org/10.1021/acs.inorgchem.5b01952.

[27] N.A. Khan, S.H. Jhung, Synthesis of metal-organic frameworks (MOFs) with microwave or ultrasound: Rapid reaction, phase-selectivity, and size reduction, Coord. Chem. Rev. 285 (2015) 11–23. https://doi.org/10.1016/j.ccr.2014.10.008.

[28] V. Trannoy, A.N. Carneiro Neto, C.D.S. Brites, L.D. Carlos, H. Serier-Brault, Engineering of Mixed Eu^{3+} /Tb^{3+} Metal-Organic Frameworks Luminescent Thermometers with Tunable Sensitivity, Adv. Opt. Mater. 9 (2021) 2001938. https://doi.org/10.1002/adom.202001938.

[29] V. Trannoy, I. N'Dala-Louika, J. Lhoste, T. Devic, H. Serier-Brault, Lanthanide Isophthalate Metal-Organic Frameworks: Crystal Structure, Thermal Behavior, and White Luminescence, Eur. J. Inorg. Chem. 2021 (2021) 398–404. https://doi.org/10.1002/ejic.202000906.

[30] X. Song, Y. Ma, X. Ge, H. Zhou, G. Wang, H. Zhang, X. Tang, Y. Zhang, Europium-based infinite coordination polymer nanospheres as an effective fluorescence probe for phosphate sensing, RSC Adv. 7 (2017) 8661–8669. https://doi.org/10.1039/C6RA27819A.

[31] L. Cunha-Silva, S. Lima, D. Ananias, P. Silva, L. Mafra, L.D. Carlos, M. Pillinger, A.A. Valente, F.A.A. Paz, J. Rocha, Multi-functional rare-earth hybrid layered networks: Photoluminescence and catalysis studies, J. Mater. Chem. 19 (2009) 2618–2632. https://doi.org/10.1039/b817381h.

[32] M. Latva, H. Takalob, V.M. Mukkala, C. Matachescu, J.C. Rodríguez-Ubis, J. Kankare, Correlation between the lowest triplet state energy level of the ligand and lanthanide(III) luminescence quantum yield, J. Lumin. 75 (1997) 149–169. https://doi.org/10.1016/S0022-2313(97)00113-0.

[33] C.D.S. Brites, A. Millán, L.D. Carlos, Lanthanides in Luminescent Thermometry, in: Handb. Phys. Chem. Rare Earths, 2016: pp. 339–427. https://doi.org/10.1016/bs.hpcre.2016.03.005.

[34] M.D. Dramicanin, Trends in luminescence thermometry., J. Appl. Phys. 128 (2020) 40902. https://doi.org/10.1063/5.0014825.

[35] X. Liu, S. Akerboom, M. De Jong, I. Mutikainen, S. Tanase, A. Meijerink, E. Bouwman, Mixed-Lanthanoid Metal-Organic Framework for Ratiometric Cryogenic Temperature Sensing, Inorg. Chem. 54 (2015) 11323–11329. https://doi.org/10.1021/acs.inorgchem.5b01924.

[36] D. Ananias, C.D.S. Brites, L.D. Carlos, J. Rocha, Cryogenic Nanothermometer Based on the MIL-103(Tb,Eu) Metal-Organic Framework, Eur. J. Inorg. Chem. 2016 (2016) 1967–1971. https://doi.org/10.1002/ejic.201501195.

[37] R.M. Abdelhameed, D. Ananias, A.M.S. Silva, J. Rocha, Luminescent Nanothermometers Obtained by Post-Synthetic Modification of Metal-Organic Framework MIL-68, Eur. J. Inorg. Chem. 2019 (2019) 1354–1359. https://doi.org/10.1002/ejic.201900110.

[38] J. Rocha, D. Ananias, F. Almeida Paz, L.D. Carlos, Near-Infrared Ratiometric Luminescent Thermometer Based on a New Lanthanide Silicate, Chem. - A Eur. J. 24 (2018) 11926–11935. https://doi.org/10.1002/chem.201802219.

SYNOPSIS. La-MOF built upon 1,3-benzenedicarboxylic acid has been synthesized by microwave-assisted hydrothermal route, reducing the synthesis time to a few minutes. The co-doping of the MOF by small amounts of Eu^{3+} and Tb^{3+} leads to new luminescent thermometers operating in the cryogenic range.